PERIODICA POLYTECHNICA SER. EL. ENG. VOL. 34, NO. 2, PP. 123–135 (1990)

ON THE APPLICATION OF AMPLITUDE OPTIMUM FOR DIGITAL CONTROL IN ELECTRIC DRIVES

G.-H. GEITNER

Institute of Electrical Engineering
Technical University Dresden, GDR

Received March 14, 1988; Revised December 14, 1989.

Abstract

The increasing use of microcomputers for control of electric drives causes an increased interest in optimization rules for digital controllers. For industrial applications in many cases the well-known optimization procedures for analog control according to the amplitude optimum (Kessler) result in an acceptable dynamic behaviour. Basic consideration of this paper is to use the statement of this optimization for sampled-data control of electric drives. By approximation of the computed equations for controller parameter adjustment simple optimization rules are obtained again. The application of the equations and the efficacy of the controller parameters is investigated by digital simulation of the control loops and oscillograms of a real drive. An important detail of this design procedure consists in the search of a simple rectifier model to reduce the order of the overall z–transfer function for the controlled process.

Keywords: amplitude optimum, cascade control structure, rectifier model, sampled-data control.

Introduction

Due to their known advantages (ISERMANN, 1980), microcomputers are increasingly used to control electric drives. The attendant time quantization has increased the interest in optimization rules for digital controllers. Optimization processes can be divided into four groups:

a) Pseudo-continuous optimization:
The sampling mode of operation is taken into account by adding the sampling time T to the smallest time constant T_Σ and the well-known optimization procedures for analog control with amplitude optimum are applied (SCHÖNFELD, 1984).

b) Modified frequency characteristics:
logarithmic amplitude/phase characteristics (Bode diagrams) for digital controllers can be computed and implemented exactly by introducing the ν transformation (SCHÖNFELD and KRUG, 1979).

c) Amplitude optimum for digital control (KRUG, 1985).

d) Designing special digital controllers:
To this group belong e. g. controllers designed for finite settling time (GEITNER and STOEV, 1985) or time-optimized controllers (BÖTTINGER, 1982).

Compared with *c)*, *a)* has the disadvantage that

$$(T \ll \text{time constant of controlled process})$$

must hold; *b)* requires relatively complicated computations owing to the ν transformation and *d)* has a higher implementation cost. In comparison with specially designed controllers (*d*) the digital amplitude optimum often yields a satisfactory dynamic performance.

Design for Digital Amplitude Optimum

The well-known optimization rules for analog amplitude optimum are summarized in *Table 1.* The controlled process and the controller are plotted in the Laplace domain. If the sampling operation is to be handled precisely, the z-transformation must be used for digital amplitude optimum.

Table 1
Control optimization according to the amplitude optimum for analog systems

Controlled process \ Controller	$\frac{1}{pT_0}$	$\frac{1+pT_1}{pT_0}$	$\frac{(1+pT_1)(1+pT_2)}{pT_0}$
$\frac{V_S}{(1+pT_{S1})}$	$T_0 = 2V_S T_1$ $T_{AN} = 5T_1$	—	—
$\frac{V_S}{(1+pT_{S1})(1+pT_\Sigma)}$	$T_0 = 2V_S T_1$ $T_{AN} = 5T_1$	$T_0 = 2V_S T_\Sigma$ $T_1 = T_{S1}$ $T_{AN} = 5T_\Sigma$	—
$\frac{V_S}{(1+pT_{S1})(1+pT_{S2})(1+pT_\Sigma)}$	$T_0 = 2V_S(T_1+T_2)$ $T_{AN} = 5(T_1+T_2)$	$T_0 = \frac{2V_S T_1 T_2 (T_1+T_2)}{T_1^2+T_1T_2+T_2^2}$ $T_1 = \frac{(T_1^2+T_2^2)(T_1+T_2)}{T_1^2+T_1T_2+T_2^2}$	$T_0 = 2V_S T_\Sigma$ $T_1 = T_{S1}$ $T_2 = T_{S2}$ $T_{AN} = 5T_\Sigma$

Similarly to analog amplitude optimum as many derivatives as possible of the amount of the closed control circuit G_g should be zero for $\omega \to 0$. For

$$G_g(z^{-1}) = \frac{a_n z^{-n} + a_{n-1} z^{-(n-1)} + \ \dots \ + a_0}{b_m z^{-m} + b_{m-1} z^{-(m-1)} + \ \dots \ + b_0} \tag{1}$$

we obtain

$$\mid G_g \mid^2 = G_g(z^{-1}) G_g(z) = \frac{u}{v} \ , \tag{2}$$

where $G_g(z)$ is the complex conjugated function.

Because of $z^i + z^{-i} = 2\cos i\omega t$ we get:

$$\mid G(j\omega) \mid^2 = \frac{\frac{1}{2}\sum\limits_{i=0}^{n} a_i^2 + \sum\limits_{i=1}^{n} \cos i\omega T \Big(\sum\limits_{j=0}^{n-i} a_j a_{j+i} \Big)}{\frac{1}{2}\sum\limits_{i=0}^{m} b_i^2 + \sum\limits_{i=1}^{m} \cos i\omega T \Big(\sum\limits_{j=0}^{m-i} b_j b_{j+i} \Big)} \ . \tag{3}$$

Since (3) contains only cos functions, the following holds in general for $\omega \to 0$:

$$\frac{d^{2k+1}(\frac{u}{v})}{d\omega^{2k+1}} = 0 \qquad \text{for } k = 0, 1, 2 \dots \ , \tag{4}$$

and for the even derivatives of (2), as many of them can be made zero as the number of free parameters specified during design.

From the requirement for the closed loop:

$$\sum_{i=0}^{n} a_i = \sum_{i=0}^{m} b_i \ , \tag{5a}$$

and the reordering made to facilitate the computation of derivatives

$$\text{if} \qquad f(\omega) = \frac{u(\omega)}{v(\omega)} \qquad \text{and} \qquad \frac{d^x f(\omega)}{d\omega^x} \cdot v(\omega) = g(\omega),$$

$$\text{then} \qquad \frac{d^{x+1} f(\omega)}{d\omega^{x+1}} v(\omega) = \frac{dg(\omega)}{d\omega} - \frac{dv(\omega)}{d\omega} \cdot \frac{g(\omega)}{v(\omega)},$$

the following equations result for a systematic optimization with $\omega \to 0$:

$$\frac{d^2 u}{d\omega^2} = \frac{d^2 v}{d\omega^2} \qquad \text{at condition (5a) and (4)} \ , \tag{5b}$$

$$\frac{d^4 u}{du^4} = \frac{d^4 v}{dv^2} \qquad \text{at condition (5b)} \ . \tag{5c}$$

For the determination of the freely specified parameters, the following formula is obtained according to KRUG (1985), where $2k$ is the number of derivatives:

$$\sum_{i=1}^{n} i^{2k}\Big(\sum_{j=0}^{n-i} a_j a_{j+i}\Big) = \sum_{i=1}^{m} i^{2k}\Big(\sum_{j=0}^{m-i} b_j b_{j+i}\Big) , \tag{6}$$

$k = 1,2,3, \ldots$

If more than one derivative is used ($k > 1$), the coefficients $k(i)$ of the partial sums over the products $x_j x_{j+i}$ with $x = a, b$ can be simplified by substitution. *Table 2* contains the results for $n, m \leq 8$.

Table 2
Coefficients for equation (6)

$i=$ Deriv.	1	2	3	4	5	6	7	8	9
2	**1**	**4**	**9**	**16**	**25**	36	49	64	81
4		**1**	**6**	**20**	**50**	105	196	336	540
6			**1**	**8**	**35**	112	294	672	1386
8				1	10	54	210	660	1782
10					1	12	77	352	1287
12						1	14	104	546
14							1	16	135
15								1	18
16									1

The range in bold typeface is generally sufficient. However, the number of derivatives used for optimization must not exceed the specified degrees of freedom. The following structure specification for the controller has proved to be useful:

$$G_R(z^{-1}) = \frac{V_R(1 + d_1 z^{-1})(1 + d_2 z^{-2})\ldots}{1 - z^{-1}} . \tag{7}$$

Since the controlled systems in the z–domain have typical transfer functions according to equation (8),

$$G_S(z^{-1}) = \frac{\frac{n_0}{m_0}(1 + n_1 z^{-1} + n_2 z^{-2} + \ldots)}{(1 - e^{-a} z^{-1})(1 - e^{-b} z^{-1})\ldots} , \tag{8}$$

where $a = T/T1$, $b = T/T2$ and $T1, T2$ are the time constants of the controlled process, controllers described by (7) can be used to compensate

Table 3
Controller optimization according to the amplitude optimum for digital systems

Controlled process $a=\frac{T}{T_1};b=\frac{T}{T_2}$			Z-transfer function of the controlled process $F_S(Z^{-1})$	Digital "PI-controller" $F_R=\frac{V_R(1-e^{-a}Z^{-1})}{(1-Z^{-1})}$
Lag elements	N=1	$T_t=1$	$Z^{-T_t}\dfrac{1+n_1Z^{-1}+n_2Z^{-2}+\dots}{\frac{m_0}{n_0}(1-e^{-a}Z^{-1})}$	$V_R=\dfrac{\frac{m_0}{n_0}}{1+3n_1+5n_2+\dots}$
		$T_t=2$		$V_R=\dfrac{\frac{m_0}{n_0}}{3+5n_1+7n_2+\dots}$
	N=2	$T_t=1$	$Z^{-T_t}\dfrac{1+n_1Z^{-1}+n_2Z^{-2}+\dots}{\frac{m_0}{n_0}(1-e^{-a}Z^{-1})(1-e^{-b}Z^{-1})}$	$V_R=\dfrac{\frac{m_0}{n_0}(1-e^{-b})^2}{(1+e^{-b})+n_1(3-e^{-b})+n_2(5-e^{-b})+\dots}$
		$T_t=2$		$V_R=\dfrac{\frac{m_0}{n_0}(1-e^{-b})^2}{(3-e^{-b})+n_1(5-3e^{-b})+n_2(7-5e^{-b})+\dots}$

N = Number of lag elements; T_t = Dead time

linear factors $(1-e^{-x}z^{-1})$ in the z–domain, analogously with analog digital optimum. Therefore, only $k=1$ (1st derivative) of (6) is necessary to determine V_R. A similar method is possible for disturbance optimization if, as with analog digital optimum, the reciprocal numerator of G_R is used as filter denominator

$$G_F(z^{-1}) = \frac{V_F}{(1+d_1z^{-1})(1+d_2z^{-2})\dots} \, . \tag{9}$$

Accordingly, $k=2$ of (6) must also be used, since two degrees of freedom have been specified. The results computed for (6) to (9) for typical controlled systems are summarised in tabular form in (KRUG, 1985).

If only a 'digital PI controller' is specified,

$$G_R(z^{-1}) = \frac{V_r(1+d_1z^{-1})}{1-z^{-1}} \, , \tag{10}$$

the computation equations for the controller gain V_R are obtained as shown in *Table 3*. These will now be used to optimize the current and speed controller of a DC drive.

Optimization of the Current Controller of a DC Drive

The current control loop structures shown in *Fig. 1* are obtained with the following conditions:

— use of a 6-pulse bridge rectifier;
— optimization in the continuous range;
— use of averaging measuring elements.

These differ in the dead time unit or delay unit of the rectifier model selected with or without sampler. The smallest time constant T_Σ and the dead time T_t are variables. *Table 4* which contains the z–transfer function of the controlled system as well as the optimization relationships for V_R has been extended with structure 3* with $T_t = T$.

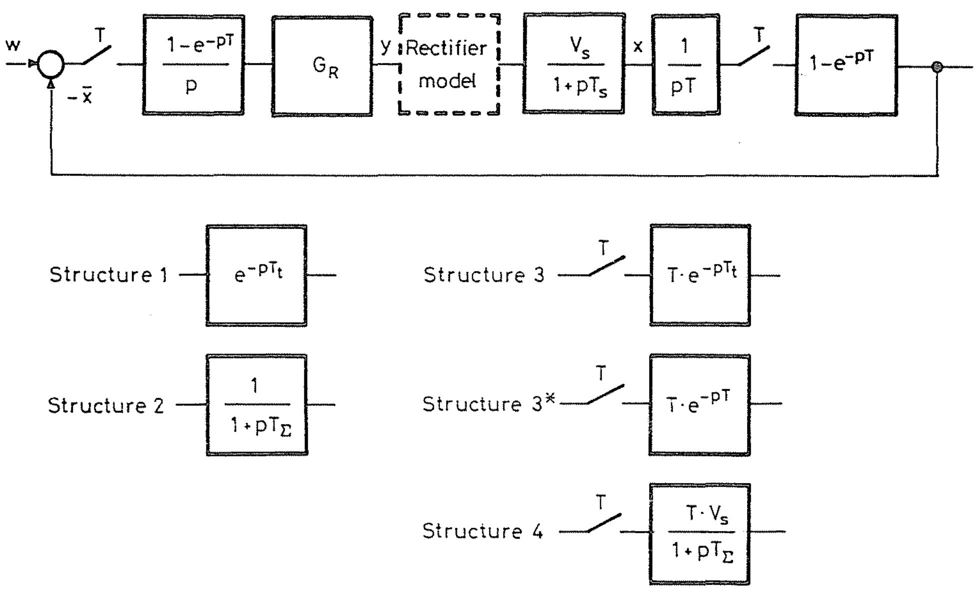

Fig. 1. Current control structures varying the rectifier model

The procedure below was followed to attain a preferred and simple model. With the value assignments $d_1 = -e^{-a} = -e^{T/T_s}$ and with the reasonable variation of

$$0 < T_t < T, \qquad 1\,\text{ms} < T_\Sigma < 4\,\text{ms} \ ,$$

a parameter range was computed for V_R for which an optimum $V_{R\text{opt}}$ was determined heuristically; this value allows a pseudo-optimum step response

Table 4
Process structure and controller dimensioning for current control structures

Rectifier approximation	Total transfer function of the controlled process	Gain of a digital PI controller with $d_1 = -e^{-a}$, $V_R \cdot V_S =$ where $\frac{m_0^*}{n_0} = \frac{m_0}{n_0} \cdot V_S$
1: Dead time unit $T_t = (1-m)\,T$ $0<m<1$	$\frac{z^{-1}(1+n_1 z^{-1}+n_2 z^{-2})}{\frac{m_0}{n_0}(1+m_1 z^{-1})}$	$\frac{m_0^*}{n_0} \cdot \frac{1}{1+3n_1+5n_2}$
2: Lag element	$\frac{z^{-1}(1+n_1 z^{-1}+n_2 z^{-2})}{\frac{m_0}{n_0}(1+m_1 z^{-1}+m_2 z^{-2})}$	$\frac{m_0^*}{n_0} \cdot \frac{(1-e^{-b})^2}{(1+e^{-b})+(3-e^{-b})n_1+(5-e^{-b})n_2}$
3: Sampler and dead time unit $T_t = (1-m)\,T$	$\frac{z^{-1}(1+n_1 z^{-1})}{\frac{m_0}{n_0}(1+m_1 z^{-1})}$	$\frac{m_0^*}{n_0} \cdot \frac{1}{1+3n_1}$
3*: Sampler and dead time unit $T_t = T$	$\frac{z^{-2}}{\frac{m_0}{n_0}(1+m_1 z^{-1})}$	$\frac{m_0^*}{n_0} \cdot \frac{1}{3}$
4: Sampler and lag element	$\frac{z^{-1}(1+n_1 z^{-1})}{\frac{m_0}{n_0}(1+m_1 z^{-1}+m_2 z^{-2})}$	$\frac{m_0^*}{n_0} \cdot \frac{(1-e^{-b})^2}{(1+e^{-b})+(3-e^{-b})n_1}$

for a large number of operating points. This optimum controller gain has been obtained with the following values: $T_t = (1-m)T$

structure 1: $m \to 1/2$,
structure 2: $T_\Sigma \to T/2$,
structure 3: $m \to 0$,
structure 3*: $T_t = T$,
structure 4: $T_\Sigma \to T$.

On this basis, the performance of the real drive was compared with the simulation results obtained for all structures at $V_R = (V_{R\text{opt}}, 1/2 V_{R\text{opt}}, 2 \cdot V_{R\text{opt}})$. Differences have been found only at very high controller gain values. It has been found that the simplest rectifier model of structure 3* with the two coefficients

$$\frac{n_0}{m_0} = V_s(1-e^{-a}) \qquad \text{and} \qquad m_1 = -e^{-a}$$

in the z–domain yields a satisfactory description of the performance of the actual closed circuit (*Figs 2a* and *b*). This statement was supported by the investigation of the stability limit: ($V_R=0.9$, $T_A=52\,\text{ms}$, $T=10/3\,\text{ms}$).

$$\text{Experimental value:} \quad V_{R\text{lim}} = 15.5$$

$$\text{Theoretical value:} \quad V_{R\text{lim}} = \frac{1}{V_s(1-e^{-a})} = 17.9\,. \tag{11}$$

With a first-order approximation of the exponential function, the computation of the controller gain for structure 3* yields the following:

$$V_R \approx \frac{T_s}{3 \cdot V_s \cdot T}\,. \tag{12}$$

A comparison with an analog amplitude optimization with the sampling mode neglected,

$$V_R = \frac{T_{R1}}{T_0} = \frac{T_s}{2V_sT_\Sigma} \tag{13}$$

shows that the same controller gain is obtained for $T_\Sigma = 1.5 \cdot T$. This corresponds to structure 2. The rectifier is described with a delay unit of 1st order with $T_\Sigma = T/2$ (see above) and the sampling mode is taken into account by adding the sampling time T to the smallest time constant. Both (13) and (12) are valid at $T_s \gg T$, the dependency of T_s appears at an approximation of the 2nd order: $T_\Sigma = 1.5T(1 - T/2T_s)$. Now we have a simple dimensioning equation based on structure 3* when performing digital amplitude optimization with the exact formula for V_R.

Speed Controller Optimization of a Simple DC Drive

For reasons of computation time and precision, the asynchronous operation of the current and speed control loop is possible. These structures can again be computed using the z–transformation if a lag element of the 1st order or a transfer function in z–domain is assumed. The theoretically computed step response of the current control loop can be used to compute the coefficients of the transfer function in z–domain with the sampling time of the speed control loop by taking into consideration the average measurement as well as to compute the time constant of the lag element (see *Fig. 2a*). The structures shown in *Fig. 3* are obtained for the speed control loop.

If the friction proportional with the speed is taken into account (feedback gain K), a lag element is obtained after the disturbance variable mixing point. The relationship with the integration time constant is $V_2=1/K$

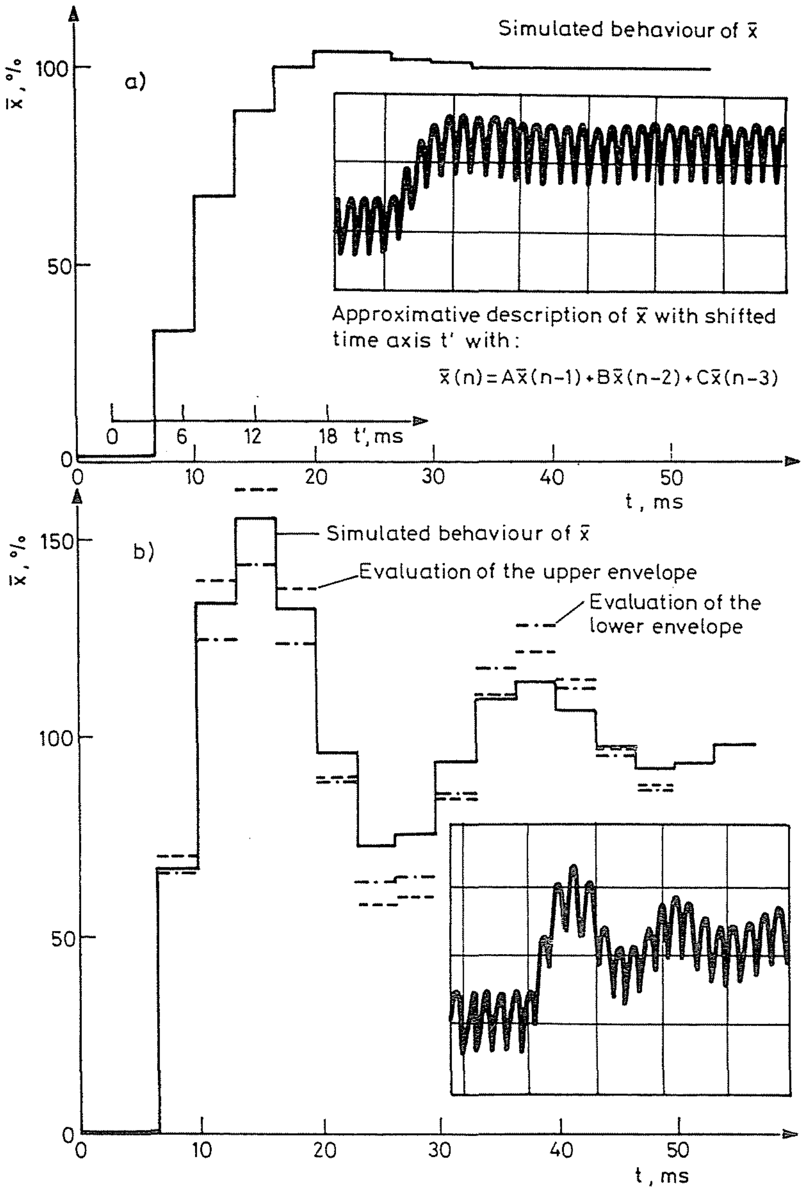

Fig. 2. Simulated step response for structure 3* and oscillogram at
a: $V_R = V_{R\text{opt}}$
b: $V_R = 2 \cdot V_{R\text{opt}}$

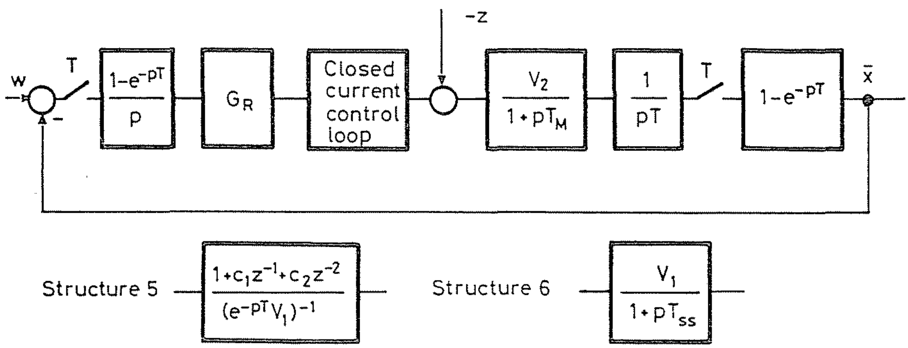

Fig. 3. Speed control structures: asynchronisation with current control loop

Table 5
Process structure and controller dimensioning for speed control structures

Current control loop	$V_1 z^{-1}(1+c_1 z^{-1}+c_2 z^{-2})$	$\frac{V_1}{1+pT_{ss}}$
Total controlled process	$\frac{z^{-2}(1+n_1 z^{-1}+n_2 z^{-2}+n_3 z^{-3})}{\frac{m_0}{n_0}(1+m_1 z^{-1})}$	$\frac{z^{-1}(1+n_1 z^{-1}+n_2 z^{-2})}{\frac{m_0}{n_0}(1+m_1 z^{-1}+m_2 z^{-2})}$
V_R of digital PI-controller	$\frac{m_0}{n_0}\cdot\frac{1}{3+5n_1+7n_2+9n_3}$	$\frac{m_0}{n_0}\cdot\frac{(1-e^{-b})^2}{(1+e^{-b})+(3-e^{-b})n_1+(5-e^{-b})n_2}$
Dependence on K	Approx. of second order $V_1\frac{m_0}{n_0}=\frac{2T_0}{T}\neq f(K)$ $n_1\approx 1+c_1, n_2\approx c_1+c_2, n_3\approx c_2$	Approx. of second order $\frac{m_0}{n_0}\approx\frac{T_0}{T}\cdot\frac{b^2}{(b^2/2+1-e^{-b}-b)}\neq f(K)$
Approx. for V_R	$=\frac{T_0}{T\cdot\lambda}$ $\lambda=4V_1(1+\frac{3}{2}c_1+2c_2)$	$\approx\frac{T_0}{T}\cdot\frac{b(1-e^{-b})}{2b+b^2+2e^{-b}+b\frac{b-2e^{-b}}{1-e^{-b}}}$

and $T_M = T_0/K$. The process structure and the controller parameters are summarised for both structures in *Table 5*.

With an approximation of the 2nd order and the reasonable assumption of $K \leq 1$ a near independence from K is obtained for both structures. Using a transfer function in z–domain a very simple dimensioning equation is obtained for V_R in the case of the speed controller. Comparing –

in *Table 5* – the controller amplifications with the practical optimum amplifications obtained with an adaptation program we find that the results for structure 6 converge from the aperiodic side and those of structure 5 from the oscillating side from V_{Ropt}. Therefore, when fixing T_Σ for a lag element, the value $i \approx i_{\text{command}}$ should be used as a starting point instead of 95% of the final value.
The performance of the real closed control loop was compared at $V_R \leq V_{Ropt}$ with the simulation results for structures 5 and 6 (see *Fig. 4*). Both models can be used in practice. Similarly to V_R, the real step response is somewhere in between the two models.

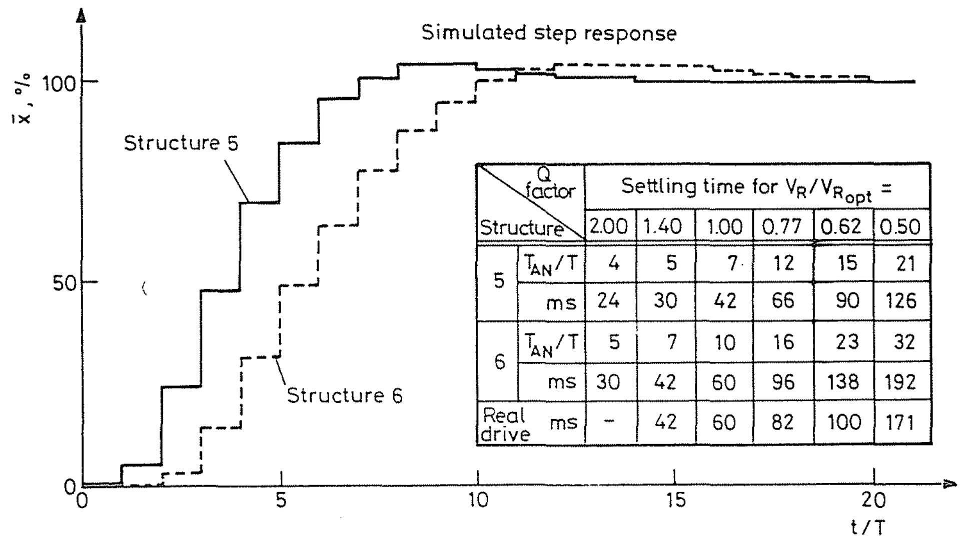

Structure \ Q factor		Settling time for $V_R/V_{R_{opt}}$ = 2.00	1.40	1.00	0.77	0.62	0.50
5	T_{AN}/T	4	5	7	12	15	21
	ms	24	30	42	66	90	126
6	T_{AN}/T	5	7	10	16	23	32
	ms	30	42	60	96	138	192
Real drive	ms	–	42	60	82	100	171

Fig. 4. Simulated step responses for structures 5 and 6 and evaluation of the oscillograms

Summary

The structures considered were simulated using a programmable pocket calculator and the following differential equations (a variation of (14)):

Controlled process:

$$\overline{x}(n) = -m_1\overline{x}(n-1) - m_2\overline{x}(n-2) + \frac{n_0}{m_0}\Big(y(n-1) + n_1 y(n-2) + n_2 y(n-3)\Big) . \tag{14}$$

Mixing point:

$$x_w(n) = w(n) - \overline{x}(n) \ . \tag{15}$$

Controller:

$$y(n) = y(n-1) + V_R[x_w(n) + d_1 x_w(n-1)] \ . \tag{16}$$

The computation equations for digital amplitude optimum have thus been investigated for 6 different structures. The fact that parameter sensitivity is comparable to that for analog amplitude optimum has been demonstrated in KRUG and GEITNER (1985). In addition to this, the present paper compares the implementation cost and the maximum dynamic actuating variable with those of EEZ controllers. The following holds for all current control loop models:

$$'T_t' = T_{tHG} + T_t + T_\Sigma \approx T = 3.3\,\mathrm{ms}\,, \tag{17}$$

if we take into account that a sampler disconnects the controlled process and the hold unit, thus eliminating the dead time $T_{t\mathrm{hold}} = T/2$ of the latter. The simplest relationships using digital amplitude optimum for basic digital control loops for DC drives with 6 pulse rectifiers are summarised below:

Current control:

$$d_1 = -e^{-\frac{T_{st}}{T_s}} \approx \frac{T_{st}}{T_s} - 1\,, \tag{18a}$$

$$V_R \approx \frac{T_s}{3V_s T_{st}}\,, \tag{18b}$$

Speed control (asynchron.):

$$d_1 \approx \frac{T_{Dr} \cdot 0.1}{T_0} - 1\,, \tag{18c}$$

$$V_R \approx \frac{T_0}{\lambda T_{Dr}} \qquad \text{with} \qquad \lambda = 4(A + \frac{3}{2}B + 2C)\,. \tag{18d}$$

with T_{st}: sampling time of the current control loop; T_{Dr}: sampling time of the speed control loop.

These equations can be used as a basis for assigning initial values of adaptation programs.

References

BÖTTIGER, A. (1982): Ein Vergleich zwischen zeitoptimaler Steuerung und Steuerung innerhalb einer gegebenen Einstellzeit. (Time-optimized control and control within a specified settling time — a comparison). *Regelungstechnik*, Vol. 30, No. 4, pp. 127–133. (in German)

GEITNER, G.-H. - STOEV, A. (1985): Optimiert auf endliche Einstellzeit. (Optimized for finite settling time.) *Messen-Steuern-Regeln*, Vol. 28, No. 2, pp. 60–65; Vol. 28, No. 4, pp. 165-169; Vol. 28, No. 5, pp. 211–214. (in German)

ISERMANN, R. (1980): Einsatz von Mikrorechnern in der Regelungstechnik. (Application of microcomputers in control systems). *Elektronik*, Vol. 29. No. 6. pp. 79–84; p. 91. (in German)

KRUG, H. (1985): Betragsoptimum für digitale Regler von elektrischen Antrieben. (Amplitude optimum for digital controllers of electric drives.) *Messen-Steuern-Regeln*, Vol. 28, No. 9, pp. 394–399. (in German)

KRUG, H.- GEITNER, G.-H. (1985): Some remarks to the optimization of digital controllers for electric drives. *5th Power Electronics Conference,* Budapest, Proceedings Part I/A. pp. 23–34.

SCHÖNFELD, R. - KRUG, H. (1979): Berechnung digitaler Regelstrukturen mit Hilfe modifizierter Frequenz-kennlinien. (Computation of digital control structures using modified frequency characteristics). *Messen-Steuern-Regeln*, Vol. 22, No. 4. pp. 186–191. (in German)

SCHÖNFELD, R. (1984): Grundlagen der automatischen Steuerung — Leitfaden und Aufgaben aus der Elektrotechnik. (Basics of automatic control — Introduction and exercises.) Berlin, VEB Verlag Technik. (in German)

Address:

Dr.-Ing. Gert-Helge GEITNER
TU Dresden, Sektion Elektrotechnik
DDR-8027 Dresden
Mommsenstr. 13.
German Democratic Republic